Neuronal Cell Adhesion Molecules and Cytotactin Are Colocalized at the Node of Ranvier

Francois Rieger,* Joanne K. Daniloff,‡ Martine Pincon-Raymond,* Kathryn L. Crossin,‡ Martin Grumet,‡ and Gerald M. Edelman‡

*Groupe de Biologie et Pathologie de la Santé et de la Recherche Médicale, Paris, France; and
‡The Rockefeller University, New York 10021

Abstract. Immunocytochemical methods were used to show that Ng-CAM (the neuron–glia cell adhesion molecule), N-CAM (the neural cell adhesion molecule), and the extracellular matrix protein cytotactin are highly concentrated at nodes of Ranvier of the adult chicken and mouse. In contrast, unmyelinated axonal fibers were uniformly stained by specific antibodies to both CAMs but not by antibodies to cytotactin. Ultrastructural immunogold techniques indicated that both N-CAM and Ng-CAM were enriched in the nodal axoplasm and axolemma of myelinated fibers as well as within the nodal regions of the myelinating Schwann cell. At embryonic day 14, before myelination had occurred, small-caliber fibers of chick embryos showed periodic coincident accumulations of the two CAMs but not of cytotactin, with faint labeling in the axonal regions between accumulations. Cytotactin was found on Schwann cells and in connective tissue. By embryonic day 18, nodal accumulations of CAMs were first observed in a few medium- and large-caliber fibers. Immunoblot analyses indicated that embryonic to adult conversion of N-CAM and a progressive decrease in the amount of Ng-CAM and N-CAM occurred while nodes were forming. Sciatic nerves of mouse mutants with defects in cell interactions showed abnormalities in the distribution patterns and amount of Ng-CAM, N-CAM, and cytotactin that were consistent with the known morphological nodal disorders. In trembler (*+/Tr*), intense staining for both CAMs appeared all along the fibers and the amounts of N-CAM in the sciatic nerve were found to be increased. In mice with motor endplate disease (*med/med*), Ng-CAM and N-CAM, but not cytotactin, were localized in the widened nodes. Both trembler and *med/med* Schwann cells stained intensely for cytotactin, in contrast to normal Schwann cells which stained only slightly. All of these findings are consistent with the hypothesis that surface modulation of neuronal CAMs mediated by signals shared between neurons and glia may be necessary for establishing and maintaining the nodes of Ranvier.

THE node of Ranvier is a highly differentiated, periodic annular narrowing (1.5–2.5 μm) interrupting the myelin sheath in myelinated axons (22). It has a privileged role in axonal conduction of the nerve impulse: membrane depolarization leads to inward current only at the nodes and conduction is saltatory between them (31, 48). Both Na^+ channels (44) and Na^+/K^+ ATPase (53) are concentrated in the nodal region; it is thus distinct in structural, functional, and molecular composition from the myelinated internodal region (150–300 μm long), which consists of a spiral Schwann cell membrane surrounding the axon (18, 33, 35, 50).

In nodal development, a single motile Schwann cell becomes associated with a growing axon, ensheaths a single internode, acquires a basal lamina, stops dividing, and begins spiral growth and myelin formation (22). Nodes may be structurally and physiologically predetermined before they achieve complete ultrastructural and physiological differentiation (47, 51). The unique function, ultrastructural specialization, and linear periodicity of the node and its determination by only a few cell types, make the molecular basis of its periodicity a particularly fascinating problem in one-dimensional pattern formation.

Because node formation involves close apposition and interaction of Schwann cell and neuron, it is reasonable to suspect that molecular mechanisms of cell adhesion play a central and early role in determining subsequent signals and localizations. We have identified two neuronal cell adhesion molecules (CAMs),[1] neural CAM (N-CAM) and neuron–glia CAM (Ng-CAM) (13–16), with widespread and characteristic distributions within the central and peripheral nervous systems (7, 10, 49). The properties of these CAMs suggest that they may play decisive roles in developmental processes of pattern formation (16). N-CAM is a cell surface glycoprotein (29) that mediates adhesion by a homophilic mechanism; i.e., an N-CAM molecule on one cell interacts

1. *Abbreviations used in this paper*: CAM, cell adhesion molecule; E, embryonic day; N-CAM, neural CAM; Ng-CAM, neuron–glia CAM.

with an N-CAM molecule on an apposing cell (29, 30). Ng-CAM has been found on neuronal cell surfaces and mediates the adhesion of neurons to glial cells by a heterophilic mechanism (23, 24); it also mediates neuron–neuron adhesion, particularly between neurites (20, 24). In addition, we have recently identified a site-restricted extracellular matrix protein, cytotactin (25), that is involved in neuron–glia interactions and is synthesized by glia but not neurons of the central and peripheral nervous systems. The distribution of this molecule in non-neural sites during embryogenesis and during neural histogenesis is particularly prominent in areas of cell movement and it may serve a function in restricting or guiding such movement (9).

In the present study, we have searched for patterned localization of these molecules in myelinated and nonmyelinated nerve fibers with immunocytochemical methods, focusing on areas of specialized interaction between axon and Schwann cell. In myelinated nerve fibers, Ng-CAM, N-CAM, and cytotactin were strongly concentrated at the node of Ranvier; in contrast, Ng-CAM and N-CAM were uniformly distributed along the length of unmyelinated fibers, and cytotactin staining was weak or absent in nonmyelinating Schwann cells. During development, early coincident accumulations of Ng-CAM and N-CAM were detected from approximately embryonic day 14 (E14) in the chick embryo sciatic nerve on small nerve fibers, before myelin formation and before accumulation of cytotactin at the node. Mutant mice with disorders of myelination showed abnormalities both in distribution and in amount of the CAMs and cytotactin. Adhesive interactions between neurons and glia mediated by the CAMs and cytotactin may thus be essential for the development of patterned distributions of nodes in normal myelinated fibers.

Materials and Methods

Animals and Biochemical Procedures

White Leghorn chickens (3–6 wk old) and chicken embryos (E14–20), 8-wk-old C57Bl/6J mice, mouse embryos (E18), and young mice (postnatal days 0, 2, 4, and 8) were used. Trembler (*+/Tr*) mice were adults; mice with motor endplate disease (*med/med*) were 3 wk old. Adult chickens were anesthestized with chloral hydrate (400 mg/g body weight); mice and all embryos were sacrificed by cervical dislocation. For biochemical analyses, sciatic nerves were removed and stored frozen at −70°C until used. Proteins were extracted in 0.5% Nonidet P-40/PBS (pH 7.4)/1 mM EDTA/250 U/ml Trasylol (Mobay Chemical Corp., Pittsburgh, PA) for analysis of N-CAM and Ng-CAM. From this extract, equal amounts of protein were resolved by SDS gel electrophoresis, transferred to nitrocellulose paper, and immunoblotted as described previously (24). The results were visualized by autoradiography.

Light Microscopic Techniques

Sciatic nerves were lightly fixed in situ with a few drops of fixative (2.5% paraformaldehyde/0.02% glutaraldehyde/0.1 M phosphate buffer [pH 7.2]) on the exposed nerve for 10 min. After removal, nerves were immersed in the same fixation solution for 40 min and either sectioned and processed for immunohistology as described (10), or teased apart for whole-mount preparations. Fine watchmakers forceps (No. 4; Drummond Scientific Co., Broomall, PA) were used to separate axon bundles and single axon preparations which were then incubated with primary and secondary antibodies.

Polyclonal and monoclonal antibodies prepared against chicken brain N-CAM (29), Ng-CAM (23), cytotactin (9, 25), and mouse N-CAM (6) were used. Polyclonal antibodies against mouse Ng-CAM were prepared by injecting rabbits with Ng-CAM isolated from detergent extracts of mouse brain membranes by affinity chromatography; immunoblot analysis showed that the antisera recognized Ng-CAM polypeptides of M_r 200,000, 135,000, and 70–80,000 (23, 24). Monoclonal antibodies against chicken brain N-CAM, anti-N-CAM No. 1 (29), anti-N-CAM No. 2 (7, 29), and 10F6 (anti-chicken brain Ng-CAM; 23, 24) were also used. Monoclonal antibody 72-38 (obtained from Drs. M. Lazdunski and J. Barhanin; Institut de Biochimie du Centre National de la Recherche Scientifique, Nice, France) was used to label voltage-dependent Na^+ channels (2, 23). This antibody has been shown to cross-react with mouse and, to a much less extent, with chicken Na^+ channel proteins (Rieger, F., J. Barhanin, M. Pincon-Raymond, C. Mourre, and M. Lazdunski, unpublished observations). Polyclonal antibodies raised against bovine brain S-100 protein were used to label Schwann cells (11) and monoclonal antibodies raised against the chick Pl myelin basic protein (from Dr. A. Peterson; Montreal General Hospital, McGill University, Montreal, Quebec) were used to differentiate myelinating and nonmyelinating Schwann cells (38). Additional staining controls included nonimmune rabbit IgG for both whole mount preparations and sections; staining for CAMs was eliminated by preincubation with the appropriate antigen. Rhodamine-conjugated monoclonal antibodies to Thy-1 (52) were obtained from Miles Scientific Div., Miles Laboratories, Inc. (Naperville, IL). Double-labeling experiments were performed as described using a mixture containing a polyclonal and monoclonal antibody (24). In all figures, double-labeled sections are indicated by a prime after the letter. Photomicrographs were taken with a Zeiss photomicroscope equipped for observation of fluorescein and rhodamine fluorescence and phase-contrast optics.

Electron Microscope Techniques

Tissues were fixed in 4% paraformaldehyde/0.1 M phosphate buffer (pH 7.4), 2 h at 4°C, incubated in increasing concentrations of sucrose (5, 10, and 20%), embedded in Tissue-Tec (Miles Scientific Div., Miles Laboratories), frozen and sectioned (5 μm) in a cryotome. These sections were then fixed for 15 min in 4% paraformaldehyde, washed twice in PBS/0.1 M glycine, and incubated in PBS/4% ovalbumin. After overnight incubation in primary antibody diluted in PBS/4% ovalbumin, sections were washed three times, and incubated with colloidal gold (5-μm particles) conjugated to protein A (Janssen Life Sciences Products, Beerse, Belgium) for 2 h. The sections were then washed three times with PBS and fixed in 2.5% glutaraldehyde/0.5% tannic acid in PBS for 1 h at 4°C; after washing three more times in PBS, the sections were postfixed in osmium tetroxide, dehydrated, and embedded in Epon. The size of the gold particles was dictated by their ability to diffuse into the section using this method; penetration was significantly lower with larger particles. Ultrathin sections were cut and observed on a Philips EM400 electron microscope. Gold particles are easily identified as symmetric solid circles using a 10× magnifying lens.

Results

To determine the distribution of Ng-CAM and N-CAM on myelinated axons of adult mouse and chicken, we examined teased fiber preparations stained with an anti-CAM antibody and antibody to the Na^+ channel to identify the nodal regions (Fig. 1). Nodes of Ranvier were also identified morphologically using phase-contrast microscopy. Colocalization of Ng-CAM (Fig. 1 *a*) and N-CAM (Fig. 1 *b*) with Na^+ channels (Fig. 1, *a'* and *b'*) at the nodal gap was observed in mouse nerves (Fig. 1, *a* and *b*). In preparations of adult chicken nerves, Ng-CAM (Fig. 1 *c*) and N-CAM (Fig. 1 *c'*) were also colocalized with Na^+ channels (not shown) at the nodes of Ranvier. In the internodal regions, 5–20 μm of the external side of the Schwann cell on each side of the nodes of Ranvier was faintly stained for both Ng-CAM and N-CAM. Staining for the Na^+ channels was also observed on Schwann cells extending away from the node (Fig. 1 *b'*), in accord with recent electrophysiological data obtained on cultured Schwann cells (5). Small-caliber fibers stained uniformly for Ng-CAM and N-CAM along their entire length (Fig. 1, *a* and *b*). Slight differences in morphology between chicken and mouse nodal regions occur because axon di-

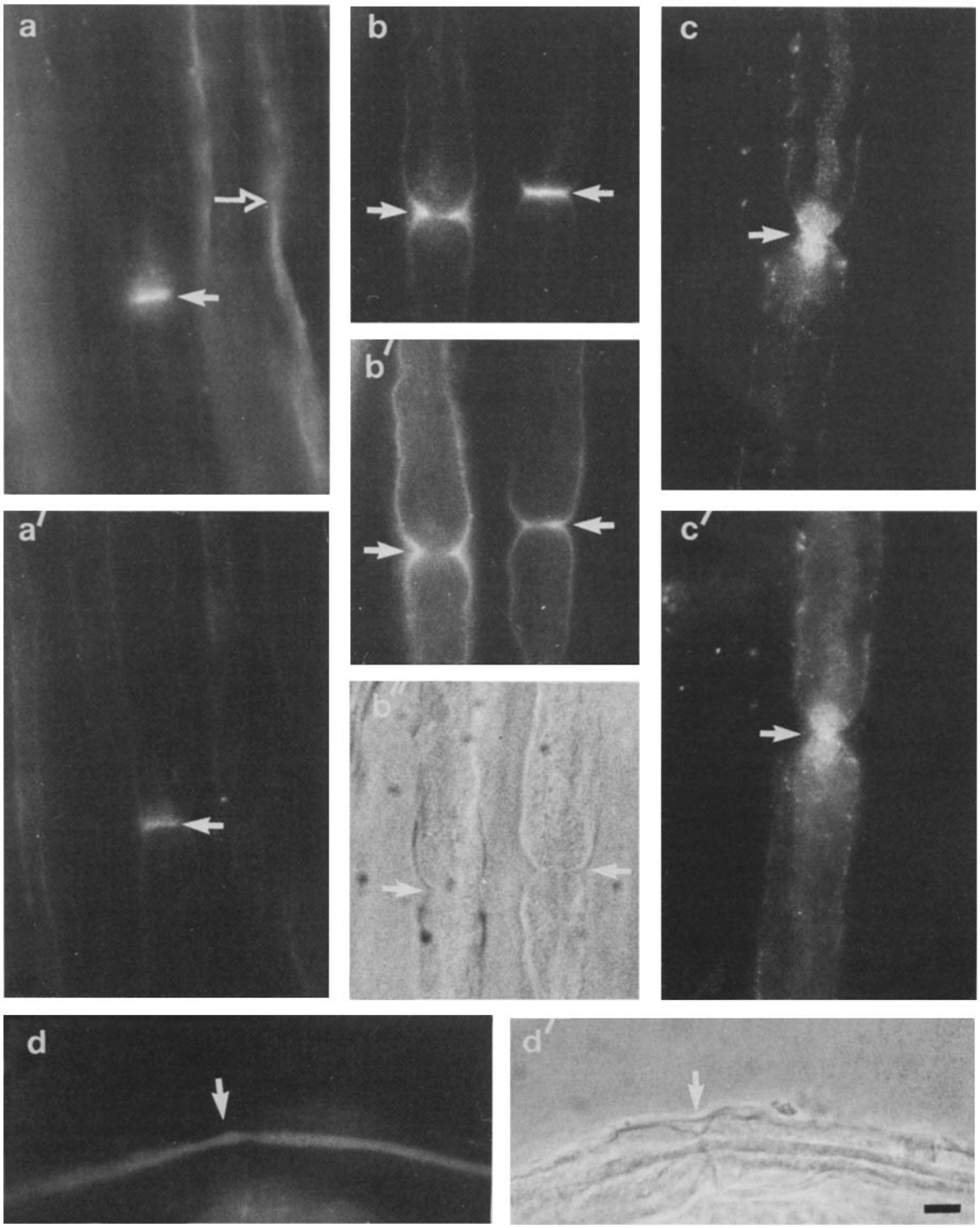

Figure 1. Coincidence of Ng-CAM and N-CAM staining at the node of Ranvier in whole-mount preparations of myelinated fibers of adult mice and chickens. All fibers shown in this figure were the largest caliber fibers in the respective preparations. In mouse sciatic nerves, the distribution of Ng-CAM (*a*) overlapped with accumulations of sodium channels (*a'*) at nodes of Ranvier (*filled arrows*). Nonmyelinated fiber bundles (*broken arrow*) were also labeled with anti-Ng-CAM antibodies. The distribution of N-CAM (*b*) was also colocalized with sodium channels (*b'*) at morphologically identified nodes of Ranvier (*b''*; phase-contrast microscopy). In teased preparations of adult chicken sciatic nerves, intense staining for both Ng-CAM (*c*) and N-CAM (*c'*) was observed at the nodal regions (*filled arrows*). Anti-Thy-1 antibodies stained the entire axon in chicken sciatic nerves (*d*) and did not accumulate exclusively at identified nodes of Ranvier (*d'*; phase-contrast microscopy; *filled arrows*). Bar, 10 μm.

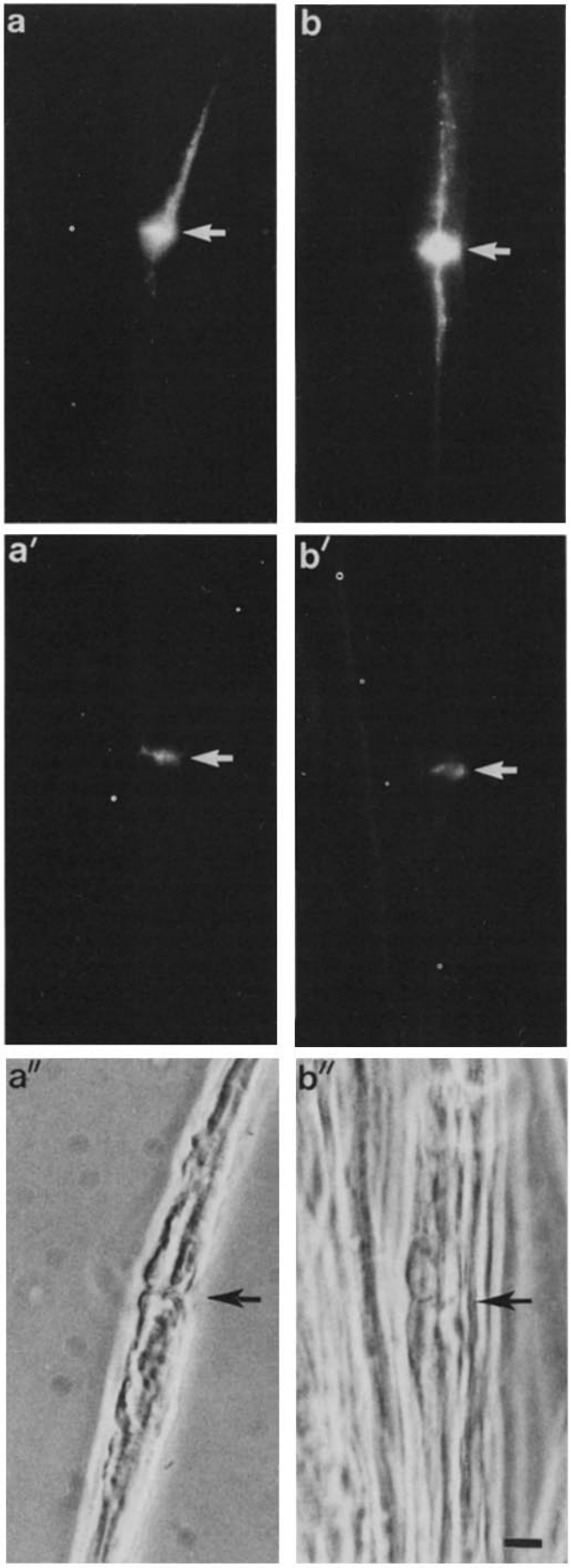

ameters are not equivalent and the width of the node is proportional to the axon diameter (42).

To ensure that the absence of staining in internodal regions was not due to blockade of surface sites by close apposition of the Schwann cell membrane, we studied the distribution of the neuronal surface marker Thy-1 (45, 52). Staining of this axolemmal protein was homogeneous all along the axonal surface, with no accumulation in the node of Ranvier region both in chick fibers (Fig. 1, *d* and *d'*) and in mouse fibers (not shown). These observations are consistent with the interpretation that the localization of CAMs at the nodes of Ranvier reflected restricted distribution of the CAMs as had previously been shown for Na^+ channel antibodies (44) and not an artifact resulting from Schwann cell–axon interactions in internodal regions or from the absence of myelin at the nodes.

Cytotactin staining was intense at the node of Ranvier (Fig. 2, *a* and *b*). Cytotactin staining was also present at what appeared to be the axon–Schwann cell interface near the nodal region, and decreased progressively in a characteristic spindle-shaped pattern as it extended away from the node. It was not detectable at internodal surfaces in myelinated axons of normal mice (Fig. 2, *a* and *b*) and chickens (data not shown). Low levels of cytotactin staining were observed at the Schwann cell surface.

Similar results were observed in longitudinal sections of adult chicken sciatic nerve (Fig. 3, *a–c*). The nodes of Ranvier, which could be identified by their characteristic morphology, were stained for both Ng-CAM and N-CAM (Fig. 3, *a* and *a'*). Ng-CAM and N-CAM were also found on the

Figure 2. Localization of cytotactin at nodes of Ranvier in whole-mount preparations of mouse sciatic nerves. Staining for cytotactin was intense in nodal regions (*a* and *b*, filled arrows), which were identified by accumulations of sodium channels (*a'* and *b'*). Nodes of Ranvier were also identified by morphologic criteria (*a"* and *b"*). Cytotactin staining extended in a characteristic spindle-shaped pattern at what appeared to be the axon–Schwann cell interface in internodal regions. Staining intensity decreased on either side of the nodes with no staining 20–30 μm from the nodes. Bar, 10 μm.

Figure 3. Longitudinal and transverse sections of adult chicken sciatic nerves stained for Ng-CAM, N-CAM, S-100, and cytotactin. Both Ng-CAM (*a*) and N-CAM (*a'*) staining was observed at nodes of Ranvier (*filled arrows*) and on the external surfaces of myelinating Schwann cells, especially in paranodal regions. Staining in a pattern reminiscent of the cross of Nageotte (34) is indicated by small arrows in *a* and *a'*. In an adjacent section (*b*), anti-S-100 staining identified Schwann cell bodies (*broken arrow*) and the external surface of myelinating Schwann cells. Cytotactin staining was intense in nodal regions (*c, filled arrow*); the outer surface of Schwann cells was also faintly labeled, especially in paranodal regions. Transverse sections at low magnification showed some faint Ng-CAM (*d*), N-CAM (*d'*), S-100 (*e*), and cytotactin (*f*) staining. The perineurium (*small arrows*) was not stained for Ng-CAM (*d*), but was N-CAM positive (*d'*). Only Schwann cells were labeled by S-100 antibodies (*e*). At higher magnification, bundles of nonmyelinated fibers (*arrowheads*) were brightly stained for both Ng-CAM (*g*) and N-CAM (*g'*). Schwann cells (*broken arrows*) that were S-100 positive (*h*) could also be identified by phase-contrast microscopy (not shown). These cells also expressed low levels of both Ng-CAM (*g*) and N-CAM (*g'*). Examination at higher magnification revealed low levels of cytotactin on Schwann cells (*i, broken arrow*) and in connective tissues between myelinated nerve bundles. Bar, 10 μm.

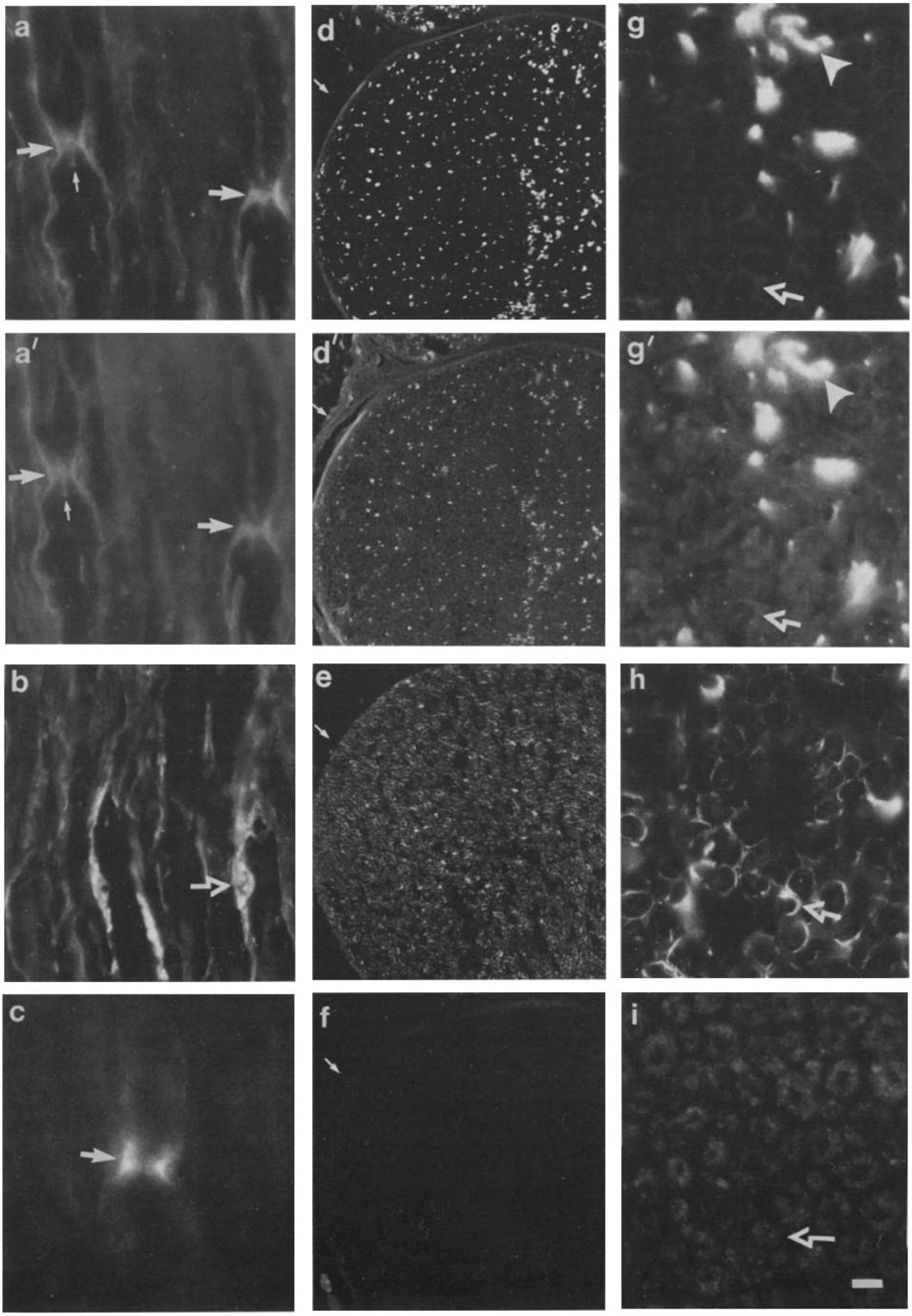
a
d
g
a′
d′
g′
b
e
h
c
f
i

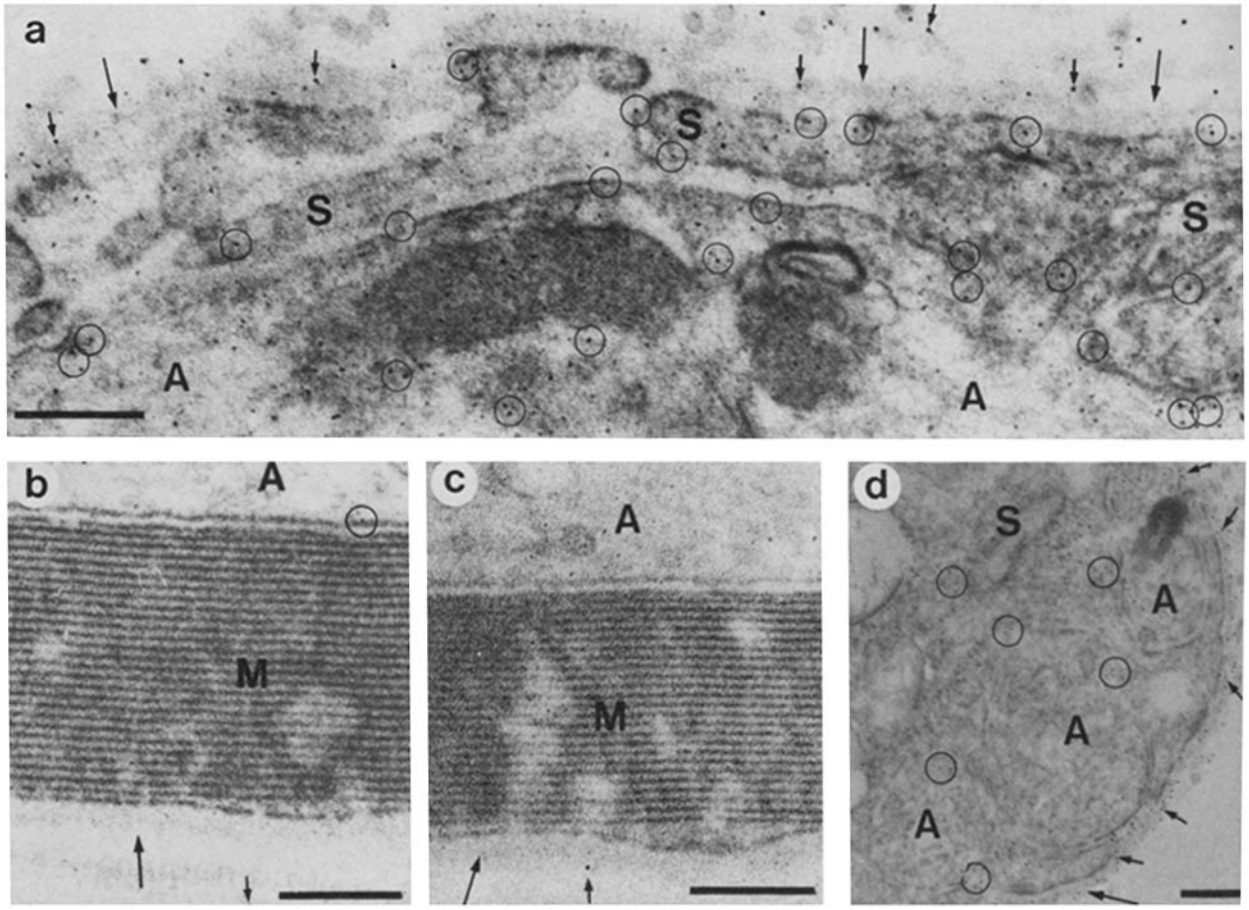

Figure 4. Ultrastructural localization of Ng-CAM in adult mouse sciatic nerves. In longitudinal sections through the node of Ranvier (*a*), staining was observed on the cell surface both of the axon and of the Schwann cell. The Schwann cell basal lamina (*large arrows*) and the cytoplasm of the terminal digitations of the Schwann cell (*S*) showed a dense distribution of Ng-CAM. (*circles*, intracellular and surface particles; *small arrows*, extracellular particles.) At the region of the node, the axoplasm also contained large numbers of colloidal gold particles (*circles* within region labeled *A*). In internodal regions (*b* and *c*), colloidal gold particles (*circles*) were much less abundant and were predominantly seen on collagen fibrils and basal lamina (*large arrows*). Particles were seen less frequently within the myelin (*M*) lamellae and the axoplasm. In a transverse section of a nonmyelinated fiber bundle (*d*), Ng-CAM staining was observed on Schwann cell and axon surfaces as well as in the cytoplasm of both cell types. Staining was most intense in the basal lamina (*large arrows*) of the nonmyelinating Schwann cell. Bars, 0.2 μm.

surfaces of myelinating Schwann cell bodies identified by S-100 staining (Fig. 3 *b*). Little or no staining was seen on the axonal membrane or in axoplasm in the internodal regions in a variety of longitudinal sections at various sites and in different planes of sectioning. Cytotactin also was found at the nodes of Ranvier in longitudinal sections (Fig. 3 *c*) and showed a distribution consistent with its presence on Schwann cell processes flanking the nodal region. Transverse sections were examined to compare the staining patterns of these molecules in myelinated and nonmyelinated axons (Fig. 3, *d–i*). Nonmyelinated axons are predominantly small-caliber fibers gathered in small bundles and scattered within the nerve; these fibers stained for both Ng-CAM (Fig. 3, *d* and *g*) and N-CAM (Fig. 3, *d'* and *g'*). As observed for myelinating Schwann cells, low levels of staining for both Ng-CAM and N-CAM were found on the S-100 positive nonmyelinating Schwann cell bodies. In cross sections, no cytotactin staining was observed on axons (Fig. 3 *f*), but faint staining occurred on Schwann cells in association with the myelin (Fig. 3 *i*).

To provide the higher resolution necessary to identify subcellular localizations, we used immunogold methods with electron microscopy. In a longitudinal section through the node of Ranvier (Fig. 4 *a*), Ng-CAM was observed at the axon cell surface and within the axoplasm in the nodal region. Staining was also apparent at the Schwann cell surface and cytoplasm, and in the basal lamina of the myelinating Schwann cell. In the heavily myelinated internodal regions

Figure 5. Transverse sections of embryonic chicken sciatic nerves at embryonic days 14 and 18. The area within the box is presented at higher magnification to the right of each low magnification micrograph. At low magnification, bundles of nonmyelinated fibers were intensely stained for Ng-CAM (*a*); the perineurium (*small arrows*) was not stained. Bundles of nonmyelinated axons (*arrowheads*) were intensely Ng-CAM positive (*b*), and Schwann cells associated with the bundles were faintly labeled (*broken arrow*). In the same section, N-CAM staining was more diffuse (*a'*) than Ng-CAM staining; bundles of nonmyelinated fibers (*arrowheads*) and Schwann cells (*broken arrow*) were also labeled (*b'*). At E14, no staining with anti-Pl myelin basic protein antibodies was observed (*c* and *d*). The perineurium

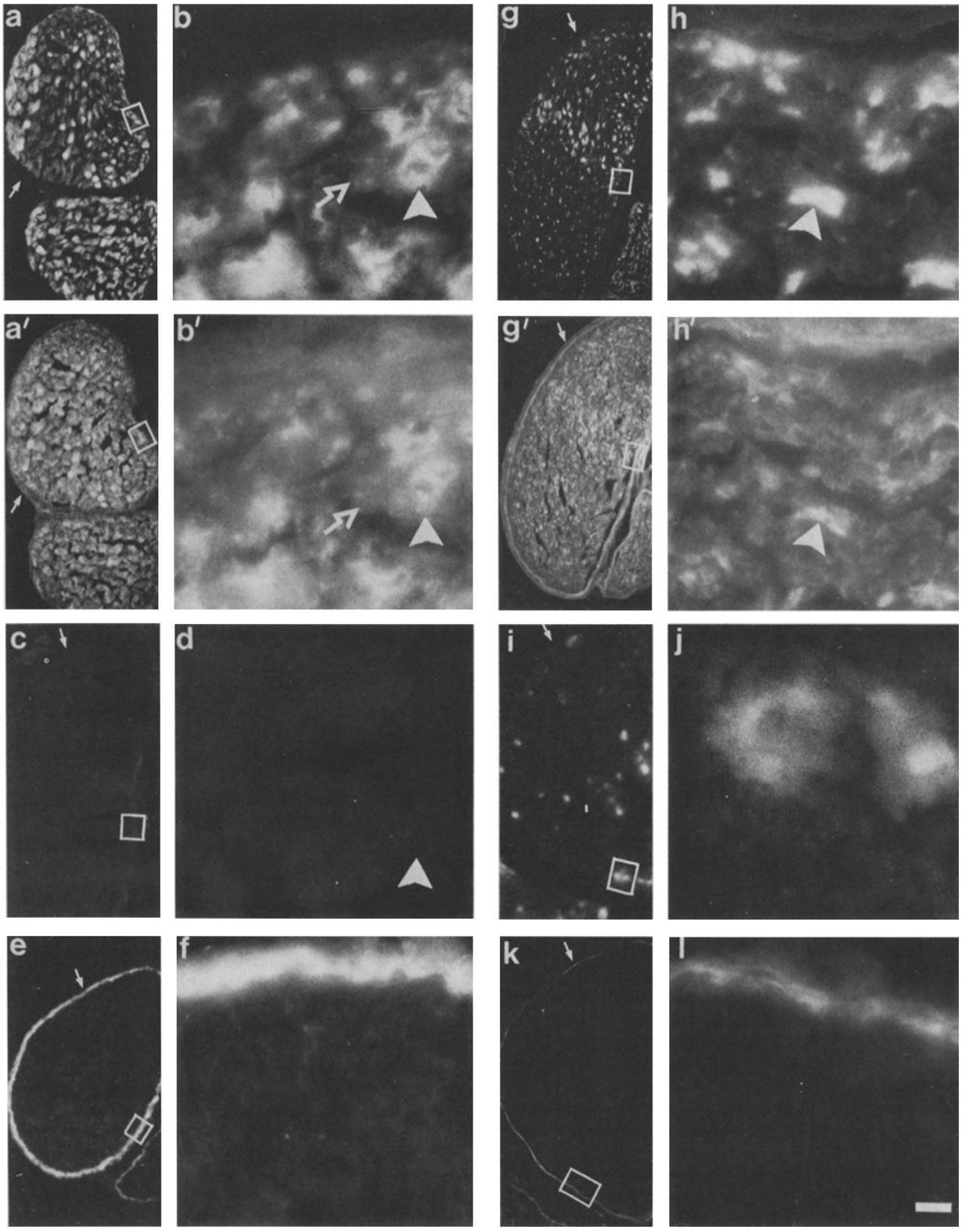

was brightly stained for cytotactin (*e*); at higher magnification (*f*), low levels of cytotactin staining were also observed within the nerve. By E18, however, the overall intensity of Ng-CAM staining (*g* and *h*) decreased while bundles of fibers (*arrowheads*) continued to express high levels of Ng-CAM (*h*). The perineurium (*small arrows*) does not express Ng-CAM. The intensity of N-CAM staining (*g'* and *h'*) also decreased. Staining in the perinurium (*small arrows*) was similar to that seen at E14. Bundles of nonmyelinated fibers continued to express high levels of N-CAM (*arrowhead*) and Schwann cells expressed lower levels (*h'*). Also at E18, some myelination occurred, as indicated by the PI staining (*i* and *j*). The perineurium (*small arrows*) continued to express cytotactin (*k* and *l*), although less intensely than at E14 (compare *e* and *f* with *k* and *l*). Bar: (*b, b', d, f, h, h', j,* and *l*) 5 μm; (*a, a', c, e, g, g', i,* and *k*) 60 μm.

(Fig. 4, *b* and *c*), staining for Ng-CAM occurred at lower levels in the axoplasm and basal lamina of the Schwann cell and in association with collagen fibrils (Fig. 4 *c*). Sections incubated with nonimmune antibodies showed a uniform low background of gold particles in both nodal and internodal regions. Examination of nonmyelinated fibers showed a more extensive distribution of Ng-CAM, consistent with results from light microscopy (Fig. 4 *d*). Particles specific for Ng-CAM were present on the Schwann cell basal lamina in a denser distribution than on myelinated fibers; they were present on the surfaces both of axons and Schwann cells, in the Schwann cell cytoplasm, and less frequently in the axoplasm. Similar results were obtained for N-CAM although the overall intensity was lower.

Developmental Distribution of CAMs and Cytotactin during Node Formation

To assess the contribution of these molecules during the development and formation of nodes of Ranvier, we examined the sequential appearance of CAMs and cytotactin on developing cellular structures related to the node of Ranvier in chick embryos. The overall distribution of Ng-CAM, N-CAM, and cytotactin was observed in cross sections of embryonic chicken sciatic nerves at E14 and E18 (Fig. 5). Ng-CAM and N-CAM overlapped in their distribution at E14 (Fig. 5, *a*, *a'*, *b*, and *b'*), and staining intensities for both CAMs significantly decreased between E14 (Fig. 5, *a*, *a'*, *b*, and *b'*) and E18 (Fig. 5, *g*, *g'*, *h*, and *h'*). Although cells resembling Schwann cells were occasionally observed at E14, the P1 myelin basic protein was rare (Fig. 5, *c* and *d*); P1 began to appear in a few areas by E18 (Fig. 5, *i* and *j*). Cytotactin staining was not present in these locations but was intense in the perineurium at E14, diminishing somewhat by E18. Some endoneurial connective tissue staining was also present (Fig. 5, *e*, *f*, *k*, and *l*).

The appearance of the P1 myelin basic protein between E14 and E18 prompted us to examine whether the periodic colocalization of Ng-CAM and N-CAM depended upon myelination. We examined teased nerve fibers from embryonic chicken sciatic nerves at various embryonic ages (E14,16, and 18) before and during the appearance of the first myelin lamellae, an event that occurs at E13–14 in 3–4% of fibers with diameters of 1 μm or greater, but which is not observed until E15–16 for thinner fibers of <1 μm (Usson, Y., and R. Saxod, Université Scientifique et Médicale de Grenoble, Grenoble, France; personal communication). Before any myelin sheaths could be detected ultrastructurally or immunocytochemically with anti-P1 antibodies, axons were already present with definite periodic accumulations of Ng-CAM and N-CAM staining (three to four successive accumulations were observed on a few 0.3–0.5 μm diameter unmyelinated axons) (Fig. 6, *a* and *a'*). Most of the other axons present at E14 showed high levels of Ng-CAM and N-CAM staining along their entire length. At E16, fibers with coincident accumulations of Ng-CAM and N-CAM were more frequent (data not shown), and were generally restricted to small areas 1–2 μm long. At E18, medium and large diameter axons with detectable myelin basic protein were observed frequently in teased preparations (Fig. 6 *b'*). These axons showed nodal accumulations of Ng-CAM (Fig. 6 *b*) and N-CAM (not shown) that contrasted sharply with otherwise

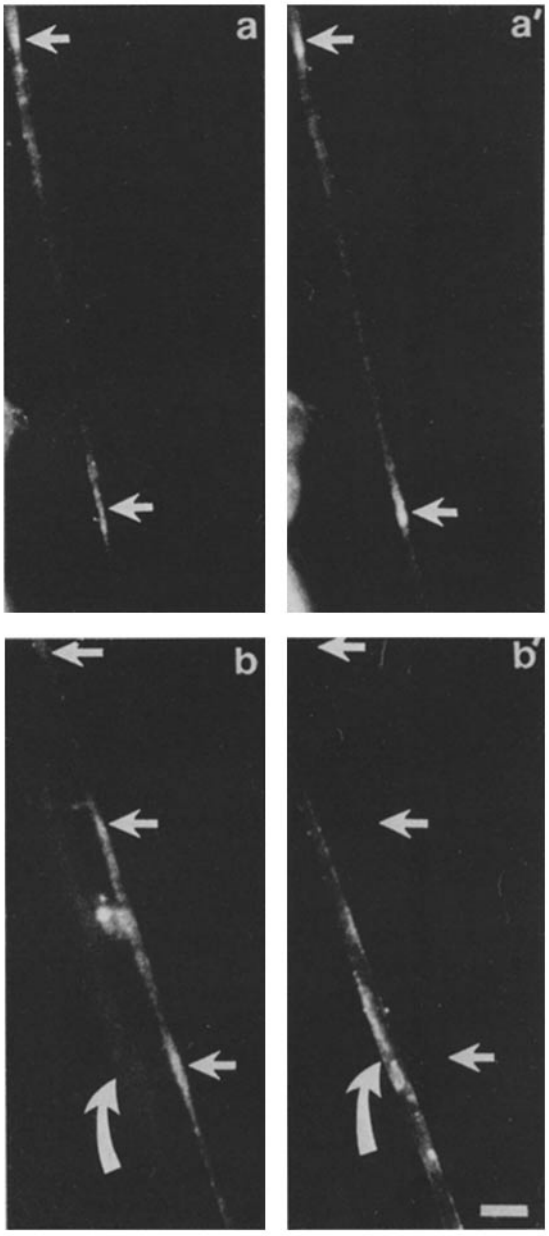

Figure 6. Teased nerve fibers from embryonic chick nerves. Early focal accumulations (*arrows*) of both Ng-CAM (*a*) and N-CAM (*a'*) were observed on teased small-caliber (0.4–0.6 μm) fibers at E14. At E18 (*b* and *b'*), focal accumulations of Ng-CAM (*b*) were found more frequently. One small fiber, of approximately the same size as that in *a*, showed Ng-CAM accumulations (*arrows* in *b*); this fiber was not myelinated, as indicated by the absence of P1 staining (*arrows* in *b'*). An adjacent fiber of larger diameter (~2 μm; *curved arrow*) was myelinated as indicated by P1 staining (*b'*), but did not have accumulations of Ng-CAM (*b*). Bar, 10 μm.

low internodal staining (Fig. 6, *a* and *b*). No accumulations of cytotactin were seen at these times (not shown).

To correlate these findings with those on more mature fibers and with studies of dysmyelinating mutants (see below), we analyzed the form and relative amounts of the CAMs in developing sciatic nerves. Ng-CAM was present mainly as a 135,000-mol-wt component that decreased in amount during development (Fig. 7 *a*). N-CAM was present

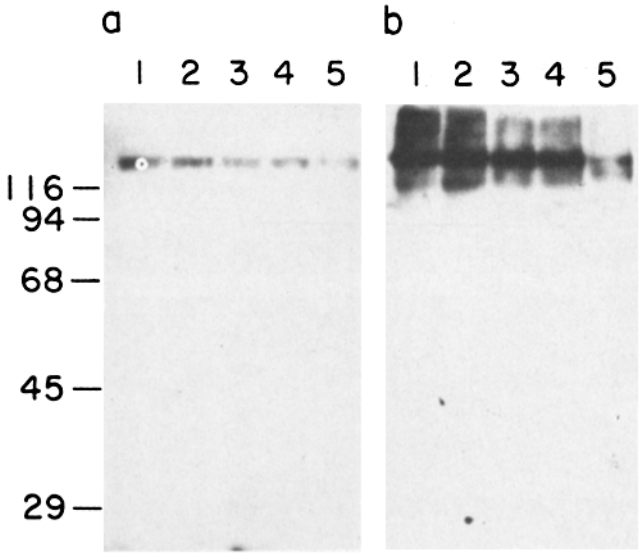

Figure 7. Immunoblot analyses of proteins extracted from normal embryonic and adult nerves. Each gel lane contains equivalent amounts of protein (50 μg) that were resolved on 7.5% polyacrylamide gels. Samples of sciatic nerve taken from E14 (lanes *1*), E16 (lanes *2*), E18 (lanes *3*), E20 (lanes *4*), and adult (lanes *5*) were immunoblotted with antibodies to Ng-CAM (*a*) and N-CAM (*b*). Migration of standard proteins is indicated by their molecular weights × 10^{-3}.

in chick embryo sciatic nerves as a polydisperse protein in the M_r 120–250,000 range (Fig. 7 *b*); it decreased sharply in amount between hatching and adulthood and began the embryonic to adult conversion (7, 17) between E16 and E18, at times when nodes are forming. In mouse sciatic nerve, this conversion has been found to occur postnatally (7). In contrast, levels of cytotactin appeared to be similar between E16 and adult (not shown). Thus, relative to total protein the amounts of CAM, but not cytotactin, decreased as their distribution became more and more localized.

Abnormal Patterns of Ng-CAM, N-CAM, and Cytotactin Staining in Mouse Mutants with Disorders of Myelination

To reveal further correlations between the staining patterns and Schwann cell–axon interactions, we studied two mouse mutants with dysmyelinating genetic disorders occurring early in development. In trembler (*+/Tr*), a rare dominant mutation, Schwann cells are the primary targets of the mutation and form significantly lower amounts of myelin than normal (1, 8). In addition, ensheathment of axons is curtailed and there is continued myelination and demyelination, as well as enhanced Schwann cell proliferation (4, 31, 37, 40). In motor endplate disease (*med/med*), nodes of Ranvier are abnormally wide as soon as myelination starts, but internodal regions are normal in length and myelin thickness (41). It is not known whether this mutation is a motorneuron or Schwann cell abnormality (42). Immunoblot analyses by SDS PAGE of normal mouse, trembler, and *med/med* sciatic nerve extracts (Fig. 8) showed that N-CAM was present as two components of M_r 120,000 and 140,000, as previously found in normal mouse nerves (43). While N-CAM was present in characteristic forms, the amounts of N-CAM as compared with normal age-matched controls were significantly elevated in trembler nerves (Fig. 8, lanes *1* and *2*) but were similar or slightly decreased in *med/med* nerves (Fig. 8, lanes *3* and *4*).

The colocalization of Ng-CAM and N-CAM at nodal regions seen in normal mouse nerves (Fig. 1) was seldom seen in trembler nerves (Fig. 9, *a* and *a'*); when present, it always occurred on small-caliber fibers. In some demyelinated nerve fibers, N-CAM staining was faint or nonexistent. Trembler fibers showed a striking abnormality consisting of patches of coincident Ng-CAM and N-CAM staining distributed all along the fiber. In *med/med* mutants, most of the nodal accumulations of Ng-CAM and N-CAM were found over a region which was wider than normal (Fig. 9, *b* and *b'*); this agrees with the previously demonstrated enlargement of nodal regions in these mutants (42). Occasionally in *med/med* nerve fibers, paranodal accumulations of both Ng-CAM and N-CAM were found separated by a gap that showed diminished staining (Fig. 9 *c*).

The distribution of cytotactin was also altered in both trembler and *med/med* mutants (Fig. 10). In trembler, Schwann cells were intensely stained for cytotactin. Faint staining was also observed all along the axon–Schwann cell interface (Fig. 10 *a*). In *med/med* nodes, staining for the Na^+ channel in small-caliber fibers was similar to normal (Fig. 10 *b*), however, no spindle-shaped accumulations of cytotactin were observed at the nodes (Fig. 10 *b'*). Moreover, cytotactin staining over the entire axon–Schwann cell interface was very prominent (Fig. 10 *b'*), and Schwann cell bodies (Fig. 10 *c*) were also brightly stained.

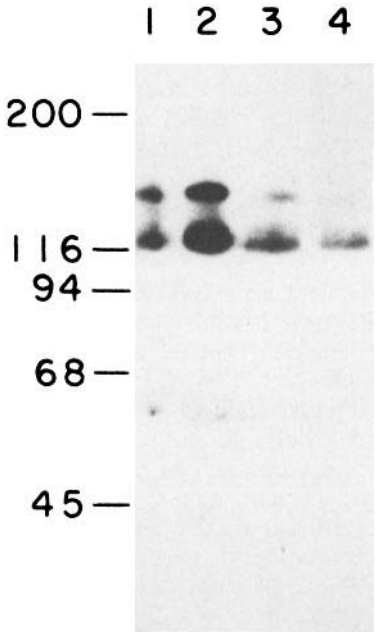

Figure 8. Immunoblot analyses of proteins extracted from normal and mutant mouse sciatic nerves. N-CAM immunoblots of extracts of trembler (lane *2*) and *med/med* (lane *4*) sciatic nerves were compared with normal age-matched controls (lanes *1* and *3*, respectively). Gel lanes contained equivalent amounts of proteins (100 μg) that were resolved on 6.0% polyacrylamide gels. Migration of standard proteins is indicated by their molecular weights × 10^{-3}.

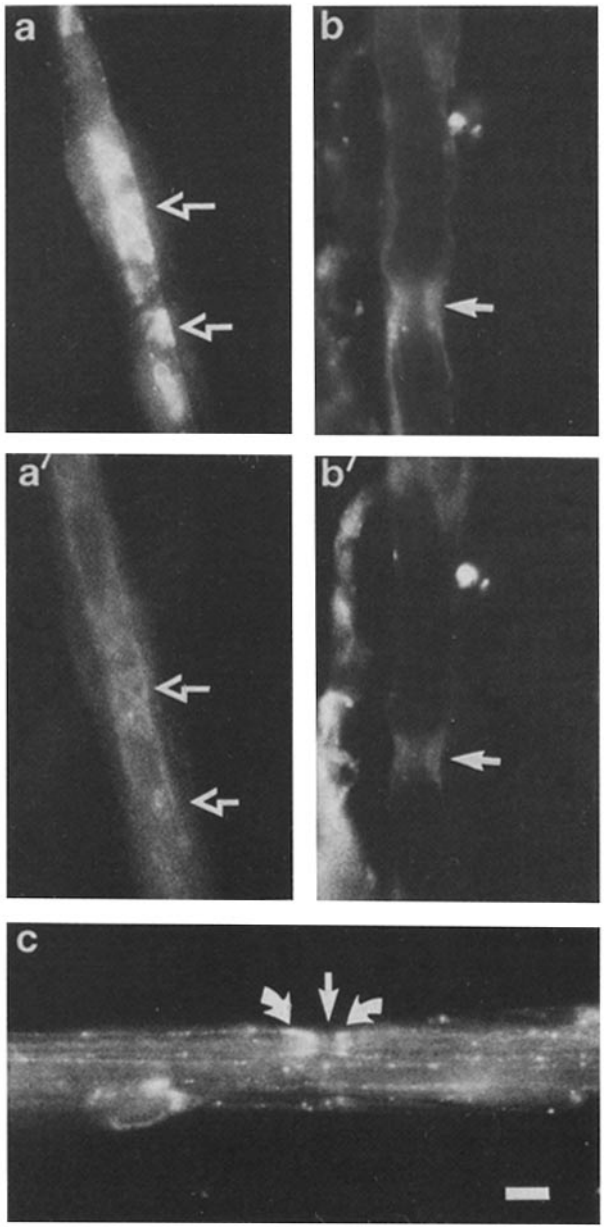

Figure 9. Abnormalities of Ng-CAM and N-CAM distributions in mutant mouse nerve fibers. In trembler (*a* and *a'*), nodal accumulations were rarely found, however, Ng-CAM and N-CAM staining patterns were generally coincident. Most of the axons showed punctate or speckled staining (*broken arrows*) for Ng-CAM (*a*) and N-CAM (*a'*). In *med/med* nerves (*b*, *b'*, and *c*), nodes of Ranvier (*arrow*) were often wider than normal, but stained for both Ng-CAM (*b*) and N-CAM (*b'*). In a small proportion of nerve fibers (*c*), paranodal accumulations (*curved arrows*) were observed with no central nodal staining for either Ng-CAM (*c*) or N-CAM (not shown). Internodal axonal staining was also elevated in these fibers. Bar, 10 μm.

Discussion

The main findings of the present study are as follows: (*a*) In myelinated peripheral nerve fibers of adult animals, Ng-CAM, N-CAM, and cytotactin were concentrated at nodes of Ranvier that were identified both by their characteristic morphology and by the accumulation of Na^+ channels. In

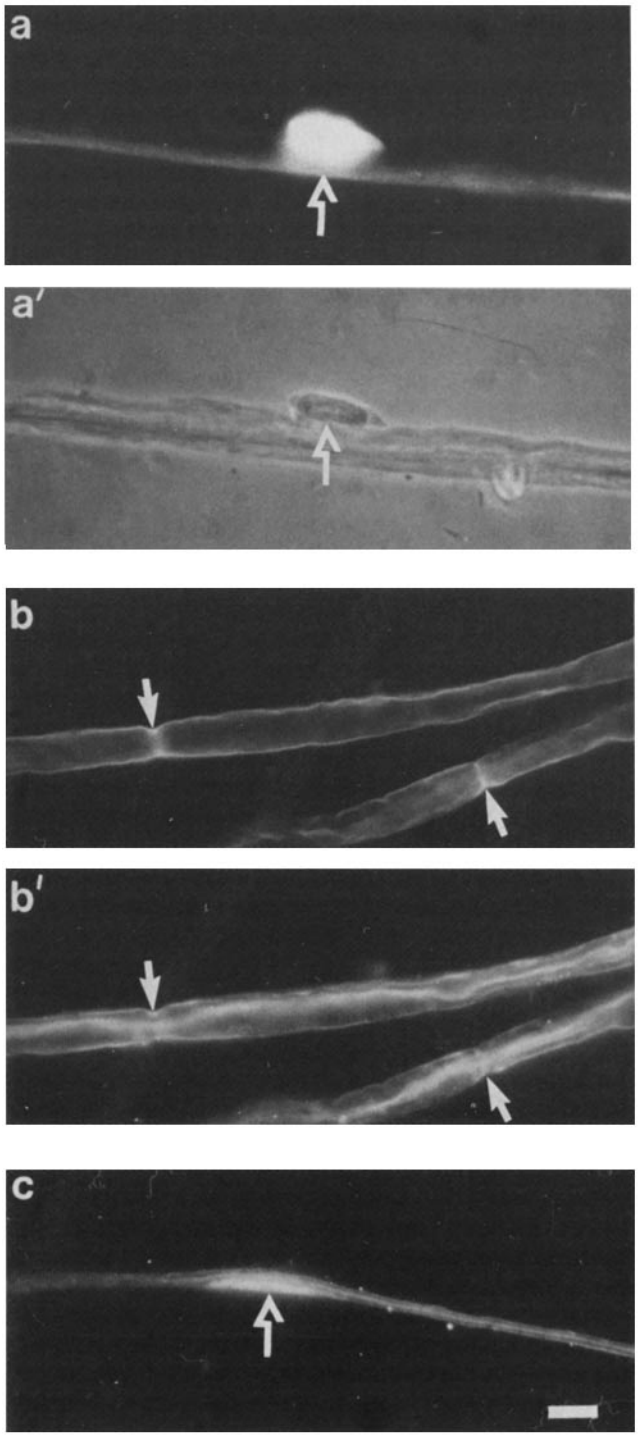

Figure 10. Localization of cytotactin in whole-mount preparations of *+/Tr* and *med/med* sciatic nerves. In *+/Tr* nerves, Schwann cells (*broken arrows*) were intensely stained for cytotactin (*a*) and were identified morphologically using phase-contrast microscopy (*a'*). Staining was also observed all along the axon–Schwann cell interface. In *med/med* nerves, antibodies to Na^+ channels (*b*) accumulated at nodes of Ranvier (*arrows*). In the same section, no significant accumulation of cytotactin was observed at the nodes (*arrows* in *b'*), although cytotactin antibodies labeled the interface between axon and Schwann cells. Schwann cells were also intensely labeled with cytotactin in this mutant (*c*, *broken arrow*). Bar, 10 μm.

internodal regions, Ng-CAM, N-CAM, and cytotactin were present in significantly lower amounts. (*b*) In contrast, nonmyelinated axons showed relatively uniform staining for Ng-CAM and N-CAM along their entire length; cytotactin staining was weak or absent in the nonmyelinating Schwann cells. (*c*) At the ultrastructural level, Ng-CAM was found on the surfaces both of axons and of Schwann cells (myelinating and nonmyelinating). This molecule was also found in the basal lamina of both Schwann cell types and in significant amounts in the cytoplasm of the axon and Schwann cell near the node. (*d*) During development, early local accumulations of Ng-CAM and N-CAM (but no corresponding cytotactin) were found on small-caliber nerve fibers as early as E14, before extensive myelination had occurred. These accumulations may possibly specify sites of formation of the nodes of Ranvier. (*e*) Genetic disorders with disturbances in axon–Schwann cell interactions show abnormal patterns of distribution of the two neuronal CAMs and cytotactin.

The presence of both CAMs at high levels only at nodes of Ranvier in myelinated fibers contrasts sharply with their uniform presence along the entire surface of unmyelinated fibers. Myelinated axons show saltatory conduction from node to node by means of accumulations of voltage-dependent sodium channels in the nodal regions as demonstrated by immunocytochemistry as well as electrophysiology (31, 48). Thus, the optimal function of myelinated axons is absolutely dependent upon the regional specialization of Na^+ channels within the restricted area of the node. The results presented in this study suggest a strong spatial correlation between the distribution of Ng-CAM and N-CAM and voltage-dependent Na^+ channels and raise the possibility that CAM distribution is related to the development of these functional regions within the axon.

Accumulations of Ng-CAM and N-CAM occur very early in nerve development on small diameter axons in chick sciatic nerve at times before myelin and myelin basic protein synthesis. During the same period, no cytotactin accumulations have been observed at these sites. These findings prompt the hypothesis that these precocious accumulations of Ng-CAM and N-CAM may be sites for future nodes of Ranvier; later accumulations of cytotactin may reflect nodal stabilization. Studies in the central and peripheral nervous systems (47, 50, 51) have shown that patches of nodal membranes form on axons prior to the formation of myelin or paranodal axo-glial junctions. Electrophysiological analysis has shown that discrete foci of inward current can be measured, suggesting that clusters of Na^+ channels exist on developing axons that may correspond to putative sites of future nodes of Ranvier (46). Moreover, morphological and physiological data suggest that Na^+ channels can cluster at the sites of developing nodes of Ranvier. It is not yet clear whether these accumulations represent "prenodes" (18) and whether these "prenodal" regions are excitable. Whatever the conclusion, the present findings open the possibility that CAMs may show localization on axonal fibers (polarity modulation) and nodal determination prior to actual myelination. To provide further evidence for this hypothesis, it will be necessary to search in the developing peripheral nerve for possible colocalization of CAMs with early Na^+ channel clusters and for a patterned relationship with adherent Schwann cells. Preliminary experiments in young mouse sciatic nerves (Rieger, F., M. Pincon-Raymond, J. Barhanin, M. Lazdunski, and G. M. Edelman, manuscript in preparation) using double-labeling of Na^+ channel protein and CAM indicate that both Na^+ channels and CAMs appear in local accumulations before myelination at approximately the same time, between birth and postnatal day 2.

These distributions bear upon the question of what factors restrict certain molecules and not others to the nodal regions. Several surface modulation mechanisms have been postulated (12–16), all of which may contribute to the localization of Ng-CAM and N-CAM at the nodes of Ranvier as development proceeds. The amounts of both Ng-CAM and N-CAM in chicken sciatic nerves decreased as their localization became more restricted during embryonic development. In addition, between E14 and E18, embryonic to adult conversion of N-CAM occurred. This conversion constitutes a large decrease of the amount of sialic acid of N-CAM with a concomitant increase in its binding efficacy (30). It may therefore be related to the establishment of prenodal areas by increasing N-CAM binding strength in a restricted area during development. It is also possible that direct or indirect interactions among CAMs, channel molecules (44, 53), nodal lipid components (5, 21), or their mutual interactions with the cytoskeleton may be involved. Similar phenomena may be involved in the colocalization of N-CAM and acetylcholine receptors at the motor endplate (43).

A striking finding of the present study is the presence of Ng-CAM and N-CAM in the basal lamina of both myelinating and nonmyelinating Schwann cells. High levels of Ng-CAM and N-CAM have also been observed (11) in the regenerating sciatic nerve: in the absence of the axon, CAM staining was observed in the basal lamina, possibly specifying the site of reinnervation. Moreover, basal lamina staining is most intense in unmyelinated axons; these axons also regenerate more readily (27, 39). Thus in the normal situation, the release of CAMs into the basal lamina may serve to stabilize the interactions of Schwann cells and axons within nerve fibers and may facilitate axon guidance in regenerating systems.

The presence of cytotactin at high levels only in myelinated fibers at the node of Ranvier, along with its curious pattern of localization on the Schwann cell at the node, suggests that it may be synthesized by the myelinating Schwann cell and transported towards the extremities of the Schwann cell thereby stabilizing the nodal structure.

Examination of the dysmyelinating mutants shows that abnormalities of axon–Schwann cell interactions are accompanied by corresponding alterations in the pattern of CAM and cytotactin localizations. These observations, and the finding that Schwann cells contain both CAMs and cytotactin, are consistent with the idea that the CAMs and cytotactin are actually mediating adhesion between glia and axons. In trembler, where the disorder is known to occur in the Schwann cells, few nodes are seen and the distribution of Ng-CAM and N-CAM remains more diffuse and patchy along the axon similar to their distributions early in normal development. Cytotactin is distributed all along the axon–Schwann cell interface and is increased in amount in the Schwann cell body. In *med/med*, Ng-CAM and N-CAM localize at the widened nodes known to be characteristic of the disease. In contrast, no accumulations of cytotactin are found in *med/med* nerves.

These results are consistent with the hypotheses that CAMs are important not only for early establishment of

nodal pattern but also for its maintenance at later stages, and that the role of cytotactin may be to stabilize nodal structures that have already been established by means of modulation of CAM expression. Given the known function of neuronal CAMs in neuron–neuron and neuron–glia adhesion (24) and of cytotactin in glia–neuron interactions (25), the present observations thus make a strong case for participation of the CAMs and cytotactin both in early pattern formation and in later stabilization of nodes. The finding that both CAMs are on peripheral neurons as well as on Schwann cells (confirmed by electron microscopy) strongly reinforces this view. The localization of Ng-CAM on Schwann cells was corroborated using antibodies to S-100 and P1 proteins as glial markers. These observations confirm the presence of L1 antigen (19), nerve growth factor–inducible large external glycoprotein (32), and Ng-CAM (11) on Schwann cells; Ng-CAM, L1 antigen, and nerve growth factor–inducible large external glycoprotein have recently been proven to be immunologically (20) and chemically (3) identical. N-CAM has also been reported to be on glial cells in central nervous system tissue (36). Moreover, our observation that Ng-CAM and N-CAM are also present on both myelinating and nonmyelinating Schwann cells supports a role for these molecules in initial axon–Schwann cell interactions.

The results of the present study open the key question of the mechanism by which cell adhesion affects nodal formation. Periodic colocalization of neuronal CAMs at early developmental times may be (*a*) intrinsic to neurons (e.g., related to homogeneity of axonal flow and cytoskeletal interactions); (*b*) intrinsic to Schwann cell distribution alone; or more likely, (*c*) the result of interactions between an individual Schwann cell and the axonal membrane with redistribution on both cell types of surface CAMs and cytotactin (polarity modulation). This redistribution of CAMs at two apposing cell surfaces might result in regional specialization of the adherent Schwann cell borders on the axon and may be accompanied by a down-regulation of the amounts of all three proteins in regions of close axon–Schwann cell apposition. Thus, as Schwann cell membrane extended along the axon, the resultant relatively high surface density of both CAMs in prospective nodal regions may restrict further extension and movement of Schwann cell borders along the axon and solidify the axon–Schwann cell interaction at the nodes. This lateral inhibition of the movement of Schwann cell processes could lead to a one-dimensional periodic pattern that is subsequently stabilized by cytotactin. Moreover, the continued presence of these adhesive molecules in a restricted area could help to maintain the morphology requisite for function in this system.

We thank Ms. Jane Steinberger for excellent technical assistance.

This research was funded by grants from Institut National de la Santé et de la Recherche Médicale, Centre National de la Recherche Scientifique, and Fondation pour la Recherche Médicale to Francois Rieger, and by a Senator Jacob Javits Center of Excellence in Neuroscience grant (NS-22789), United States Public Health Service grants AM-04256, HD-16550, and HD-09635, and Postdoctoral Fellowship NS-07636 to Joanne K. Daniloff.

Received for publication 5 March 1986, and in revised form 7 May 1986.

References

1. Aguayo, A. J., G. M. Bray, C. M. Perkins, and I. D. Duncan. 1979. Axon sheath cell interactions in peripheral and central nervous system transplants. *Soc. Neurosci. Symp.* 4:361–383.

2. Barhanin, J., H. Meiri, G. Romey, D. Pauron, and M. Lazdunski. 1985. A monoclonal immunotoxin acting on the Na^+ channel, with properties similar to those of a scorpion toxin. *Proc. Natl. Acad. Sci. USA.* 82:1842–1846.

3. Bock, E., C. Richter-Landsberg, A. Faissner, and M. Schachner. 1985. Demonstration of immunochemical identity between the nerve growth factor-inducible large external (NILE) glycoprotein and the cell adhesion molecule L1. *EMBO (Eur. Mol. Biol. Organ.) J.* 4:2765–2768.

4. Bray, G. M., M. Rasminsky, and A. J. Aguayo. 1981. Interactions between axons and their sheath cells. *Annu. Rev. Neurosci.* 4:127–162.

5. Chiu, S. Y., P. Shrager, and J. M. Ritchie. 1984. Na^+ and K^+ currents in rabbit cultured Schwann cells. *Soc. Neurosci. Abstr.* 10:947.

6. Chuong, C.-M., D. A. McClain, P. Streit, and G. M. Edelman. 1982. Neural cell adhesion molecules in rodent brains isolated by monoclonal antibodies with cross-species reactivity. *Proc. Natl. Acad. Sci. USA.* 79:4234–4238.

7. Chuong, C.-M., and G. M. Edelman. 1984. Alteration in neural cell adhesion molecules during development of different regions of the nervous system. *J. Neurosci.* 4:2354–2368.

8. Cornbrooks, C., M. Cochran, F. Mithen, M. B. Bunge, and R. P. Bunge. 1980. Myelination in explants of *Trembler* dorsal root ganglion grown in culture. *Trans. Am. Soc. Neurochem.* 11:110.

9. Crossin, K. L., S. Hoffman, M. Grumet, J.-P. Thiery, and G. M. Edelman. 1986. Site-restricted expression of cytotactin during development of the chicken embryo. *J. Cell Biol.* 102:1917–1930.

10. Daniloff, J. K., C.-M. Chuong, G. Levi, and G. M. Edelman. 1986. Differential distribution of cell adhesion molecules during histogenesis of the chick nervous system. *J. Neurosci.* 6:739–758.

11. Daniloff, J. K., G. Levi, M. Grumet, F. Rieger, and G. M. Edelman. 1986. Altered expression of neuronal CAMs induced by nerve injury and repair. *J. Cell Biol.* In press.

12. Edelman, G. M. 1976. Surface modulation in cell recognition and cell growth. *Science (Wash. DC).* 192:218–226.

13. Edelman, G. M. 1983. Cell adhesion molecules. *Science (Wash. DC).* 219:450–457.

14. Edelman, G. M. 1984. Modulation of cell adhesion during induction, histogenesis, and perinatal development of the nervous system. *Annu. Rev. Neurosci.* 7:339–377.

15. Edelman, G. M. 1985. Cell adhesion and the molecular processes of morphogenesis. *Annu. Rev. Biochem.* 54:135–169.

16. Edelman, G. M. 1985. Expression of cell adhesion molecules during embryogenesis and regeneration. *Exp. Cell Res.* 161:1–16.

17. Edelman, G. M., and C.-M. Chuong. 1982. Embryonic to adult conversion of neural cell adhesion molecules in normal and *staggerer* mice. *Proc. Natl. Acad. Sci. USA.* 79:7036–7040.

18. Ellisman, M. H., and S. R. Levinson. 1982. Immunocytochemical localization of sodium channel distributions in the excitable membranes of electrophoresis electricus. *Proc. Natl. Acad. Sci. USA.* 79:6707–6711.

19. Faissner, A., J. Kruse, J. Niche, and M. Schachner. 1984. Expression of neural cell adhesion molecule L1 during development in neurological mutants and in the peripheral nervous system. *Dev. Brain Res.* 15:69–82.

20. Friedlander, D. R., M. Grumet, and G. M. Edelman. 1986. Nerve growth factor enhances expression of neuron–glia cell adhesion molecule in PC12 cells. *J. Cell Biol.* 102:413–419.

21. Ganser, A., D. Kirschner, and M. Willinger. 1983. Ganglioside localization on myelinated nerve fibers by cholera toxin binding. *J. Neurocytol.* 12:921–938.

22. Geren, B. B. 1954. The formation from the Schwann cell surface of myelin in the peripheral nerves of chick embryos. *Exp. Cell Res.* 7:558–562.

23. Grumet, M., and G. M. Edelman. 1984. Heterotypic binding between neuronal membrane vesicles and glial cells is mediated by a specific cell adhesion molecule. *J. Cell Biol.* 98:1746–1756.

24. Grumet, M., S. Hoffman, C.-M. Chuong, and G. M. Edelman. 1984. Polypeptide components and binding functions of neuron-glia cell adhesion molecules. *Proc. Natl. Acad. Sci. USA.* 81:7989–7993.

25. Grumet, M., S. Hoffman, K. L. Crossin, and G. M. Edelman. 1985. Cytotactin, an extracellular matrix protein of neural and non-neural tissues that mediates glia-neuron interactions. *Proc. Natl. Acad. Sci. USA.* 82:8075–8079.

26. Hay, E. 1981. Cell Biology of Extracellular Matrix. Plenum Publishing Corp., New York. 417 pp.

27. Gutmann, E., and F. K. Sanders. 1943. Recovery of fibre numbers and diameters in regeneration of peripheral nerves. *J. Physiol. (Lond.).* 101: 489–518.

28. Hemperly, J. J., B. A. Murray, G. M. Edelman, and B. A. Cunningham. 1986. Sequence of a cDNA clone encoding the polysialic acid-rich and cytoplasmic domains of the neural cell adhesion molecule N-CAM. *Proc. Natl. Acad. Sci. USA.* 83:3037–3041.

29. Hoffman, S., B. C. Sorkin, R. White, R. Brackenbury, R. Mailhammer, U. Rutishauser, B. A. Cunningham, and G. M. Edelman. 1982. Chemical characterization of a neural cell adhesion molecule purified from embryonic brain membranes. *J. Biol. Chem.* 257:7720–7729.

30. Hoffman, S., and G. M. Edelman. 1983. Kinetics of homophilic binding by embryonic and adult forms of the neural cell adhesion molecule. *Proc. Natl. Acad. Sci. USA.* 80:5762–5766.

31. Huxley, A. F., and R. Stampfli. 1949. Evidence for saltatory conduction

in peripheral myelinated nerve fibers. *J. Physiol. (Lond.).* 108:315–339.

32. McGuire, J. C., L. A. Greene, and A. V. Furano. 1978. NGF stimulates incorporation of fucose or glucosamine into an external glycoprotein in cultured rat PC12 pheochromocytoma cells. *Cell.* 15:357–365.

33. Meiri, H., I. Zeitoun, H. H. Grunhagen, V. Lev-Ram, Z. Eshhar, and J. Schlessinger. 1984. Monoclonal antibodies associated with sodium channel block nerve impulses and stain nodes of Ranvier. *Brain Res.* 310:168–173.

34. Nageotte, M. J. 1910. Sur une nouvelle formation de la gaine de myeline; le double bracelet epineux de l'etrangement annulaire. *C. R. Acad. Sci.* (Paris). 48:123–126.

35. Neumcke, B., and R. Stampfli. 1982. Sodium currents and sodium-current fluctuations in rat myelinated nerve fibers. *J. Physiol. (Lond.).* 329: 163–184.

36. Noble, M., M. Albrechtsen, C. Moller, J. Lyles, E. Bock, C. Goridis, M. Watanabe, and U. Rutishauser. 1985. Glial cells express N-CAM/D2-CAM-like polypeptides *in vitro*. *Nature (Lond.).* 316:725–728.

37. Perkins, C. S., A. J. Aguayo, and G. M. Bray. 1981. Schwann cell multiplication in trembler mice. *Neuropathol. Appl. Neurobiol.* 7:115–126.

38. Peterson, A., and J. Marler. 1983. P1 deficiency in shiverer myelin is expressed by Schwann cells in shiverer and normal mouse chimaera nerves. *Neurosci. Lett.* 38:163–168.

39. Ramon y Cajal, S. 1928. Degeneration and regeneration of the nervous system. Vol. 1. R. M. May, translator and editor. Oxford University Press, London. 396 pp.

40. Rayburn, H. R., A. C. Peterson, and A. J. Aguayo. 1980. Development and deployment of Schwann cells in peripheral nerves of *Trembler* normal mouse chimaeras. *Soc. Neurosci. Abstr.* 6:660.

41. Rieger, F., and M. Pincon-Raymond. 1980. The motor innervation in motor endplate disease (med) in the mouse. Evidence for nerve abnormalities prior to muscle damage. *INSERM (Inst. Natl. Santé Rech. Med.) Symp.* 14:163–170.

42. Rieger, F., and M. Pincon-Raymond. 1984. The node of Ranvier in neurological mutants. *In* Advances in Cellular Neurobiology. Vol. 6. S. Federoff, editor. Academic Press, Inc. New York. 273–310.

43. Rieger, F., M. Grumet, and G. M. Edelman. 1985. N-CAM at the vertebrate neuromuscular junction. *J. Cell Biol.* 101:285–293.

44. Ritchie, J. M., and R. B. Rogart. 1977. The density of sodium channels in mammalian myelinated nerve fibers and nature of the axonal membrane under the myelin sheath. *Proc. Natl. Acad. Sci. USA.* 74:211–215.

45. Rostas, J. A. P., T. A. Shevenan, C. M. Sinclair, and P. L. Jeffrey. 1983. The purification and characterization of a Thy-l-like glycoprotein from chicken brain. *Biochem. J.* 213:143–152.

46. Smith, K. J., H. Bostock, and S. M. Hall. 1982. Saltatory conduction precedes remyelination in axons demyelinated with lysophosphotidyl choline. *J. Neurol. Sci.* 54:13–31.

47. Tao-Cheng, J. H., and J. Rosenbluth. 1983. Development of nodal and paranodal membrane specialization in amphibian peripheral nerves. *Dev. Brain Res.* 3:577–594.

48. Tasaki, I. 1939. The electro-saltatory transmission of the nerve impulse and the effect of narcosis upon the nerve fiber. *Am. J. Physiol.* 127:211–227.

49. Thiery, J.-P., A. Delouvée, M. Grumet, and G. M. Edelman. 1985. Initial appearance and regional distribution of the neuron–glia cell adhesion molecule in the chick embryo. *J. Cell Biol.* 100:442–456.

50. Waxman, S. G., and R. E. Foster. 1980. Ionic channel distribution and heterogeneity of the axon membrane in myelinated fibers. *Brain Res. Rev.* 2:205–234.

51. Waxman, S. G., J. A. Black, and R. E. Foster. 1982. Freeze-fracture heterogeneity of the axolemma of premyelinated fibers in the CNS. *Neurology.* 32:418–421.

52. Williams, A. F., and J. Gagnon. 1982. Neuronal Thy-1 glycoprotein: homology with immunoglobulin. *Science (Wash. DC).* 216:696–703.

53. Wood, J. G., D. H. Jean, J. M. Whitaker, B. J. McLaughlin, and R. W. Albers. 1977. Immunocytochemical localization of the sodium, potassium activated ATPase in knifefish brain. *J. Neurocytol.* 6:571–581.